COMMUNICATION

ChemComm
www.rsc.org/chemcomm

Synthesis of core–shell polyurethane–urea nanoparticles containing 4,4′-methylenedi-*p*-phenyl diisocyanate and isophorone diisocyanate by self-assembled neutralization emulsification†

In Woo Cheong* and Jung Hyun Kim

Yonsei Center for Nanotechnology, Yonsei University, 134 Shinchon-dong, Seodaemoon-ku, Seoul 120-749, South Korea. E-mail: chiw@yonsei.ac.kr; Fax: +82 2 312 6401; Tel: +82 2 2123 3554(28)

Received (in Cambridge, UK) 28th June 2004, Accepted 6th August 2004
First published as an Advance Article on the web 14th September 2004

Polyurethane–urea nanoparticles containing 4,4′-methylenedi-*p*-phenyl diisocyanate and isophorone diisocyanate were synthesized by utilizing self-assembled neutralization emulsification and their particle morphology could be controlled.

Aqueous polyurethane (APU) and polyurethane–urea (APUU) have been received considerable attention as versatile materials in various applications and several methods for the preparation of APU or APUU have been studied and developed for many years.[1–6] One of the most preferred methods is a prepolymer mixing process,[7–9] which consists of three steps: (1) formation of isocyanate (NCO)-terminated prepolymer; (2) neutralization and emulsification of the NCO–terminated prepolymer for particle formation; (3) chain extension for the higher molecular weights and urea-linkage formation. In this process, aliphatic diisocyanates, such as isophorone diisocyanate (IPDI) and hexamethylene diisocyanate (HDI), have frequently been used. In fact, the usage of cheap aromatic diisocyanates, such as 4,4′-methylenedi-*p*-phenyl diisocyanate (MDI) and toluene diisocyanate (TDI), has been restricted due to the high reactivity toward water molecules, which accelerates destabilization of the APUU particles by forming $–NH_2$, CO_2, –NHCONH–, and biuret linkages.[10–13] Introduction of the MDI in the IPDI–based APUU will give us both cost reduction and manifold physico-chemical properties. In this paper we report, for the first time, the synthesis and chracterization of MDI–IPDI based APUU nanoparticles having core–shell or inverted core–shell morphologies and the film properties as well.

The APUU nanoparticles having core–shell or inverted core–shell structure can be obtained by the formation of blocked amphiphilic prepolymers, *i.e.*, hydrophilic MDI–dimethylol propionic acid (DMPA) prepolymer blocks and hydrophobic IPDI–polytetramethylene adipate polyol (PTMA) prepolymer blocks, as depicted in Scheme 1. Carboxylic acid of the DMPA imparts hydrophilicity to the NCO-prepolymer of MDI–DMPA to locate in the shell part. For the core–shell (**B**) morphology, OH–terminated MDI–DMPA prepolymers (NCO/OH = 0.5) and NCO–terminated IPDI–PTMA prepolymers (NCO/OH = 2.0) were first prepared separately and then these two prepolymers are mixed to prepare NCO–terminated prepolymers (NCO/OH = 1.2). Triethylamine (TEA) was added into the reactor for neutralization, and the prepolymer was dropped into the water with high–speed stirring (rpm >500). During the dispersion, these amphiphilic prepolymers are self-assembled to form a core–shell structure. Finally, the APUU nanoparticles were obtained by addition of ethylene diamine (EDA) at room temperature. The inverted core–shell (**C**) nanoparticles were obtained by replacing MDI with IPDI in the similar way. For comparative study, the APUU nanoparticle having 50 mol% MDI (**A**, the same composition as core–shell and inverted core–shell morphologies) was synthesized by the conventional prepolymer mixing process, where both DMPA and PTMA were added together in the beginning of the polyaddition with MDI (NCO/OH = 0.6). After the formation of OH–terminated prepolymers containing MDI, IPDI was added to form NCO–terminated prepolymer (NCO/OH = 1.2) and followed by dispersion and chain extension processes.

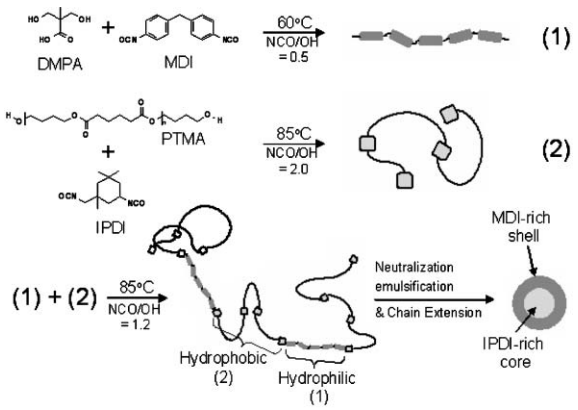

Scheme 1 Representative synthetic diagram for the APUU nanoparticles of MDI–core and IPDI–shell morphology *via* stepwise prepolymer mixing and self-assembled neutralization emulsification.

As listed in Table 1, $\bar{D}_{ls}$ and $\bar{M}_n$ of the APUUs show similar values, however, the PDI values of **B** and **C** are as twice as that of **A**. This large difference in the PDI is mainly attributed to the reactivity difference between the primary and secondary NCOs of the IPDI as well as the reactivity difference between the NCO groups of the MDI and IPDI, which is resulted from the nucleophilicity difference due to innate chemical structure.[14,15] The $\bar{D}_{ls}$ and $\bar{M}_n$ were affected by DMPA content, NCO/OH ratio, and molecular weight of the PTMA polyol.

Fig. 1 shows representative particle morphologies of the MDI–IPDI APUU nanoparticles and their wide angle X-ray diffraction (WAXD) patterns. The dark region of the particle in the photos indicates the area where the MDI molecules are predominantly localized. From **A** in Fig. 1, one can judge that the MDI molecules are delocalized all over the particle that is synthesized with the conventional prepolymer mixing process. This result seems reasonable, since no difference at the beginning of reaction was observed in the reactivity between DMPA and PTMA in the separate polyaddition reactions under *in situ* FTIR monitoring at 2273 cm^{-1} with the internal standard of $–CH_2–$ at 2964 cm^{-1}.[16] The photos **B** and **C** in Fig. 1 show the core–shell and inverted core–shell morphologies, respectively. A shadow in the vicinity of the particles in **B** and **C** is well contrast with their surrounding and core parts. Amphiphilic nature of segmented prepolymer is believed to be a driving force determining particle morphology.

WAXD patterns of the solvent–cast APUU films are shown in Fig. 1. The *d*-spacings of **A** are 4.15(α), 3.95(β), and 3.67(γ) Å, which are identical values of the PTMA. As listed in Table 1, the sample, **A** shows 21.3% crystallinity which is arising from the PTMA (*ca.* 40% crystallinity for pure PTMA). The PTMA polyol is crystallizable and known to form planar crystal structure as investigated by several researchers.[17–19] For MDI, two phenyl

† Electronic supplementary information (ESI) available: experimental details and characterizations of the MDI–IPDI nanoparticles. See http://www.rsc.org/suppdata/cc/b4/b409755f/

DOI: 10.1039/b409755f

Table 1 Basic properties of MDI–IPDI APUU nanoparticles and their solvent-cast films

Sample	$\bar{D}_{ls}$[a]/nm	ζ-pontential/mV	$\bar{M}_n$/g mol^{-1}	$\bar{M}_w$/g mol^{-1}	PDI[b] (−)	T_g/°C	T_m/°C	Crystallinity[d] (%)
A	97 ± 4	−45 ± 11	31200	54800	1.8	NA[c]	45.5	21.3
B	89 ± 2	−42 ± 9	11400	34000	2.9	−20.1	NA[c]	Amorphous
C	81 ± 2	−53 ± 13	10400	27300	2.6	−34.2	NA[c]	Amorphous

[a] The average particle measured by dynamic light scattering method. [b] Polydispersity index ($=\bar{M}_w/\bar{M}_n$). [c] Not available due to indiscernible variation. [d] Estimated from the relative areas of WAXD pattern deconvoluted by the Lorentz–Gauss method.

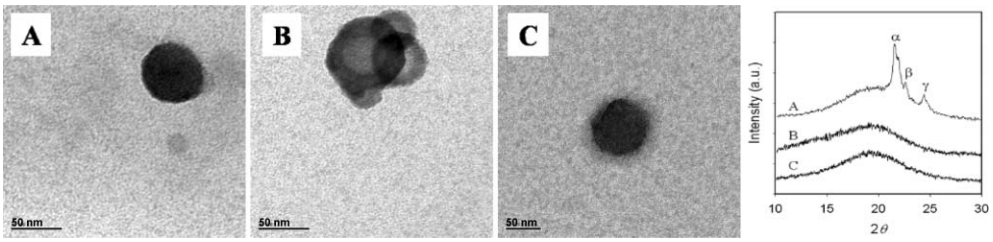

Fig. 1 Representative TEM photos of the APUU nanoparticles having (A) homogeneous composition, (B) core–shell, (C) inverted core–shell morphologies (three photos from left hand side, scale bar = 50 nm, magnification = 100k) and their WAXD patterns (on the right hand side).

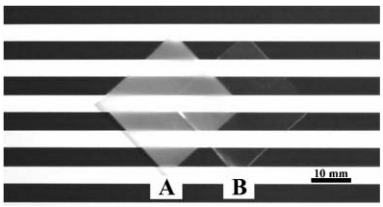

Fig. 2 Comparison of transparency between the films **A** and **B** in Fig. 1.

isocyanates are linearly connected at the pivot of the methylene group that grants flexible conformation. Thus, urethane or urea groups containing MDI molecules form well–ordered hard segment domains with strong hydrogen bond. On the contrary, IPDI consists of 75%–*trans* and 25%–*cis* isomers and its restrained chair structure probably interferes with the hydrogen bond between hard segments. Moreover, the PTMA used in this work has a long chain length (*ca.* 1000 g mol^{-1}). Thus, crystallization process of the PTMA is expected to be very favorable. No crystalline peak can be seen in the **B** and **C**. This results can be explained by predominant phase separation between hard and soft segments due to the enhanced hydrogen bonding force of longer hard segment blocks as compared with **A**. From the DSC results of **A**, a large melting peak at 46 °C was obtained but no T_g was detected due to the indiscernible transition with a wide range of temperature. No T_m was found in the DSC results of **B** and **C**, but T_g was found at −20.1 and −34.2 °C, respectively. Elastomeric property of the APUU can only be obtained when the crystalline formation of the polyester polyol is suppressed.[20] As seen in Fig. 2, the dried film (thickness = 0.13 ± 0.01 mm) of **A** shows opacity unlike **B** and **C**, since microphase separation between the hard and soft segments is not favorable. The crystallization of PTMA is certainly suppressed by hard segment interaction, since the interaction is an instantaneous process whilst the crystallization process should overcome the activation energy barrier of molecular rearrangement.

In summary, the core–shell and inverted core–shell particle morphologies of APUU nanoparticles containing MDI and IPDI could be controlled by manipulating the reaction sequence and consequent molecular rearrangement affected their film properties. Introduction of MDI in the IPDI-based APUU increases hydrogen bonding between hard segments and interferes crystal formation of the PTMA. However, the conventional prepolymer mixing process may not effectively distort crystal structure of soft segment consists of PTMA due to random distribution of DMPA in the APUU polymer backbone. On the contrary, the stepwise prepolymer method induces structured APUU nanoparticles of the amphiphilic and blocked prepolymers.

This work has been financially supported by Korea Institue of Science and Technology Evaluation and Planning (KISTEP, NRL Program: M1–99–11–000044) and Yonsei Center for Nanotechnology (YCNT).

Notes and references

1 B. K. Kim, T. K. Kim and H. M. Jeong, *J. Appl. Polym. Sci.*, 1994, **53**, 371.
2 J. F. Lee and D. Y. Chao, *Colloid Polym. Sci.*, 1994, **272**, 1508.
3 Y. S. Huang, S. L. Dong, K. H. Yang, C. P. Chwang and D. Y. Chao, *J. Coat. Technol.*, 1997, **69**, 69.
4 S. Sundar, K. Tharanikkarasu, A. Dhathathreyan and G. Radhakrishnan, *Colloid Polym. Sci.*, 2002, **280**, 915.
5 X. Wei, Y. Ying and X. Yu, *J. Appl. Polym. Sci.*, 1998, **70**, 1621.
6 T.-Z. Wang and K.-N. Chen, *J. Appl. Polym. Sci.*, 1999, **74**, 2499.
7 Y. K. Jhon, I. W. Cheong and J. H. Kim, *Colloids Surf., A*, 2001, **179**, 71.
8 I. W. Cheong, H. C. Kong, J. S. Shin and J. H. Kim, *J. Dispersion Sci. Technol.*, 2002, **23**, 511.
9 M. Lahtinen, R. K. Pinfield and C. Price, *Polym. Int.*, 2003, **52**, 1027.
10 M. Barrere and K. Landfester, *Macromolecules*, 2003, **36**, 5119.
11 F. M. B. Choutinho and M. C. Delpech, *Polym. Degrad. Stab.*, 2000, **70**, 49.
12 D. J. Hourston, G. D. Williams, R. Satguru, J. C. Padget and D. Pears, *J. Appl. Polym. Sci.*, 1999, **74**, 556.
13 S. Y. Lee, J. S. Lee and B. K. Kim, *Polym. Int.*, 1997, **42**, 67.
14 O. Lorenz, H. Decker and G. Rose, *Angew. Makromol. Chem.*, 1984, **122**, 83.
15 H. K. Ono, F. N. Jones and S. P. Pappas, *J. Polym. Sci., Polym. Lett. Ed.*, 1985, **23**, 509.
16 I. W. Cheong, H. C. Kong, J. H. An and J. H. Kim, *J. Polym. Sci. A: Polym. Chem.*, 2004, **42**, 4353.
17 T. Iwata and Y. Doi, *Macromol. Chem. Phys.*, 1999, **200**, 2429.
18 E. Pouget, A. Almontassir, M. T. Casas and J. Puiggali, *Macromolecules*, 2003, **36**, 698.
19 W. B. Liau and R. H. Boyd, *Macromolecules*, 1990, **23**, 1531.
20 S. Zhang, L. Cheng and J. Hu, *J. Appl. Polym. Sci.*, 2003, **90**, 257.